Materials & Design (2014). 55, 674-682.
DOI: http://dx.doi.org/10.1016/j.matdes.2013.10.028

Microstructural and mechanical characterisation of 7075 aluminium alloy consolidated from a premixed powder by cold compaction and hot extrusion

M.A. Jabbari Taleghani [a,b,*], E.M. Ruiz Navas [a], J.M. Torralba [a,b]

[a] Department of Materials Science and Engineering, Universidad Carlos III de Madrid, Avda. de la Universidad 30, 28911 Leganés, Madrid,
[b] IMDEA Materials Institute, C/Eric Kandel 2, Tecnogetafe, 28906 Getafe, Madrid, Spain
* Tel.: +34 91 549 34 22; fax: +34 91 550 30 47. E-mail address: mohammad.jabbari@imdea.org (M.A. Jabbari Taleghani).

Abstract: The present work concerns the processing of 7075 Al alloy by cold compaction and hot extrusion of a pre-mixed powder. To this end, a premixed Al–Zn–Mg–Cu powder, Alumix 431D, was uniaxially cold pressed at 600 MPa into cylindrical compacts 25 mm in diameter and 15 mm thick. Subsequently, selected green compacts were subjected to either a delubrication or presintering heat treatment. Extrusion of the pow-der compacts was performed at 425 °C using an extrusion ratio of 25:1. No porosity was present in the microstructures of the extruded alloys. Heat treatment prior to extrusion had a great effect on the degree of alloy development in powder compacts and, as a direct consequence, remarkably affected the extru-sion process and the as-extruded microstructures and mechanical properties of the processed materials. Hot extrusion caused banded structures for the alloys consolidated from the green and delubricated pow-der compacts. The alloy extruded from the presintered powder compact showed a fine, recrystallized microstructure which resulted in a superior combination of mechanical properties for the consolidated material.

Keywords: Aluminium alloys, Premixed powders, Powder extrusion, Microstructural characteristics, Mechanical properties.

1. Introduction

Having a superior combination of properties, such as high strength and fracture toughness [1], low density [2,3], good workability and weldability, and remarkable stress corrosion cracking resistance [4], Al–Zn–Mg–Cu alloys have long been regarded as some of the best candidates for demanding structural applications in the aerospace and automotive industries. In fact, 7xxx series Al alloys represent some of the highest strength Al alloys in commercial use [5].

Al powder metallurgy combines the superior properties of Al with the ability of powder metallurgy (PM) to produce high-performance, net- or near-net-shaped parts, thus reducing or eliminating the capital and operating costs associated with intricate machining operations. Powder extrusion (PE) is a PM processing method that has been developed for the production of fully dense, high-performance materials from powders. Compared with other PM routes such as sintering and hot pressing, the shear stresses involved in PE make it an ideal process for the production of bulk Al alloys and composites from powder mixtures. One of the main difficulties in sintering Al-based alloys is the presence of a surface oxide layer intrinsic to Al-based powders. In the case of PE, the shear stresses break the oxide layer covering the particle surfaces of these powders, leading to a well-bonded microstructure and superior after-extrusion mechanical properties [6]. According to Verlinden et al. [7], there are three methods for the extrusion of powder mixtures: loose powder extrusion, green billet extrusion, and powder extrusion using canning and degassing. The third method is mainly used for Al powders [8], but canning and degassing constitute a costly and inconvenient processing step. Consequently some researchers made efforts towards the extrusion of Al powder mixtures without canning and degassing [9,10]. These researchers directly extruded the green billets cold compacted from Al powder mixtures using a mixture of graphite and oil serving as both a lubricant [11] and an oxidation barrier [12]. They studied the microstructures and mechanical properties of the extruded products. Their promising results imply that the employed method can replace powder extrusion using canning and degassing for Al-based powders [13].

Compared with premixed Al-based powders, pre-alloyed powders are generally harder and exhibit higher flow stresses. As a result, their compressibility and hot deformability are lower than those of the premixes. In fact they are more difficult to process. Furthermore, the green density of a powder compact affects the as-extruded density and the mechanical properties of the extruded product. Song and He [14] studied the effects of die-pressing

pressure and extrusion on the microstructures and mechanical properties of SiC reinforced pure Al composites. Their results indicate that a higher green density results in a higher as-extruded density and improved mechanical properties. Thus, the lower green densities obtainable for pre-alloyed powders can reduce after-extrusion density and, as a direct consequence, negatively affect the mechanical properties of the extrusion product. In this context, the processing of fully dense Al alloys by hot extrusion using premixed Al-based powders is of great importance.

In the past decade, premixed Al-based powders have attracted great attention. These powders are ready-to-press and can be sintered to high densities through liquid phase sintering. A number of leading powder producers have addressed this interest and developed commercial premixes mainly based on high strength Al alloys. Included are Alumix 13 and 123 (2xxx series), Alumix 321 (6xxx series), and Alumix 431D (7xxx series) produced by Ecka Granules, Germany. Martin and Castro [15] studied the sintering behaviour of the mentioned premixes and reached a maximum sintered density of 97% of the theoretical value. Min et al. [16] examined the sintering characteristics of AMB 2712 (2xxx series), a commercial premixed powder produced by Ampal, USA. Their sintering processes yielded PM parts with a maximum relative density of 93%. Porosity has a very detrimental effect on the mechanical properties of PM alloys. In addition, the liquid phase sintering of Al alloys causes distortion, which is problematical to accommodate during design and to modify after sintering [17]. Therefore, development of full density, net-shaped processes and optimisation of processing parameters for the consolidation of pre-mixed Al-based powders is of great significance.

Pre-alloyed powders have been used in most of the previous works on the extrusion of Al-based powders, and studies on the extrusion of PM Al premixes are scarce. In a previous work by Zubizarreta et al. [18], Alumix 13 premix which is basically a mixture of elemental Al and Cu powders has been consolidated by hot extrusion. Although different heat treatments prior to extrusion have been performed, all of the bulk alloys processed by these researchers show banded microstructures and contain porosity and pure Cu particles, thus resulting in low hardness values for the extrusion products. Premixed powders are generally considered unsuitable for powder extrusion mainly because of the development of inhomogeneous and banded microstructures through the extrusion process, which may, however, be prevented by using a suitable premix and designing an appropriate processing route based on systematic thermal, microstructural, and mechanical characterisation of the alloys under study at different stages of the consolidation process. Considering all of the above, the present study examined the processing of 7075 Al alloy by direct hot extrusion of powder compacts cold pressed from a commercial Al–Zn–Mg–Cu premix. The main objective was to produce a bulk alloy with homogeneous microstructure and superior mechanical properties from the employed premixed powder.

2. Experimental procedure

The raw material used for this study is a commercially available premixed Al–Zn–Mg–Cu powder, Alumix 431D (Ecka Granules, Germany), with a chemical composition equivalent to 7075 Al alloy (5.6–6.4 wt% Zn, 2.4–3 wt% Mg, 1.5–2 wt% Cu, 0.1–0.3 wt% Sn, and the balance Al). The main component of this premix is atomised pure Al powder, which is mixed with a master alloy powder containing all of the alloying elements. As this mixture is a ready-to-press blend, it typically contains 1.5 wt% lubricant to facilitate the pressing step.

This premix was uniaxially cold pressed at 600 MPa into cylindrical billets 25 mm in diameter and 15 mm thick. Subsequently, selected green compacts were subjected to either a delubrication (heating to 400 °C and holding at this temperature for 20 min) or presintering (heating to 400 °C and holding at 400 °C for 20 min, followed by heating to 525 °C and soaking at this temperature for 45 min) heat treatment. The heating rate for all of the heating steps was 5 °C/min; and both heat treatments were performed in a high-purity nitrogen atmosphere. After heat treatment, the samples were furnace cooled to room temperature.

Extrusion of the powder compacts was performed at 425 °C, without caning and degassing, using an extrusion ratio of 25:1 to ensure full density after extrusion. Before heating to the extrusion temperature, a thin layer of a mixture of graphite and oil was applied to the surfaces of the powder compacts, serving as both a lubricant and an oxidation barrier. The compacts were extruded to form rods 5 mm in diameter and approximately 350 mm long. After extrusion, the extruded rods were air cooled to room temperature.

To investigate the microstructural evolution of the powder compacts during heating to extrusion temperature, selected compacts were impregnated with the graphite mixture, heated to 425 °C in air, and water quenched from this temperature.

Simultaneous thermal analysis (STA), scanning electron microscopy (SEM), X-ray diffractometry (XRD), and hardness, tension, and compression testing were employed for the microstructural and mechanical characterisation of the as-received premix, the powder compacts, and the extrudates. The reported hardness value for each material is the average value of twelve measurements. Tension and compression testing were conducted in accordance with the **ASTM: E8M** and **ASTM: E9** standards, and the number of specimens for tension and compression testing of each extruded alloy were five and three, respectively.

Both heat-treated and non-heat-treated powder compacts were sectioned parallel to the pressing direction for the microstructural and mechanical analyses. The sectioned samples were then mounted in a conductive resin, ground, and polished with diamond paste. The microstructures of the powder compacts were studied by SEM using a Philips XL30 microscope in backscattered electron (BSE) mode (accelerating voltage: 15 kV). Several samples were etched using Keller etchant prior to SEM imaging. XRD was also employed for the qualitative analysis of the phases present in the microstructure. A Philips diffractometer with Cu Kα radiation (λ = 0.15406 nm) generated at 40 kV and 40 mA was used for the XRD measurements. The XRD patterns were recorded in the 2θ range of 15–60° (step size: 0.05°, time per step: 20 s).

For the characterisation of the extruded materials, extrudates were sectioned parallel to the extrusion direction (i.e., longitudinal sections). To eliminate the possible effects of microstructural differences between different parts of the extrudates, all of the samples were cut from the middle of each extruded rod. The samples were then mounted and prepared using the same conventional metallographic techniques described above for the powder compacts. The extruded samples were characterised by SEM and XRD using the same parameters introduced before.

3. Results and discussion

3.1. Heat treatment prior to extrusion

The aim of the delubrication heat treatment was elimination of the pressing lubricant to study the effect of this lubricant on the as-extruded microstructure and mechanical properties of the consolidated alloy. Based on the STA curves presented in Fig. 1, temperatures as high as 350–400 °C are needed for complete elimination of the lubricant. Thus, heating to 400 °C and soaking at this

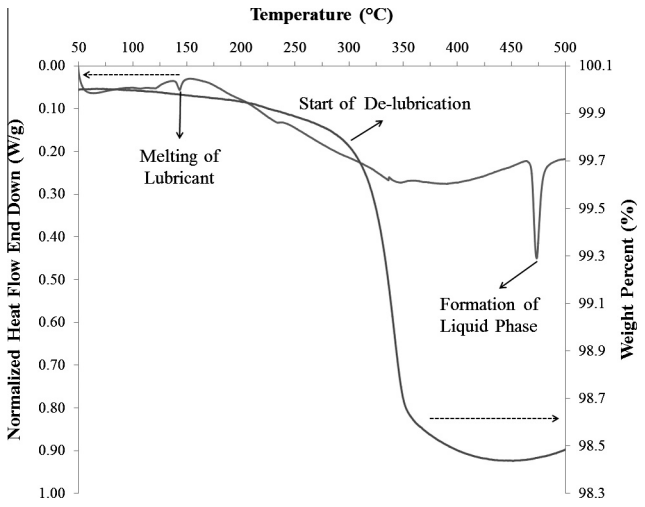

Fig. 1. Simultaneous thermal analysis (STA) of the as-received Alumix 431D powder.

temperature for 20 min was employed as the delubrication treatment.

The differential scanning calorimetry (DSC) curve in Fig. 1 shows a sharp endothermic peak at approximately 475 °C. Considering the chemical composition of the material and the temperature at which the peak appears, this peak can be attributed to low-temperature reactions between the $MgZn_2$ and/or $Al_2Mg_3Zn_3$ (also known as Mg_{32} (Al, Zn)$_{49}$ or the T phase) phases and the Al solid solution (Al (α)) matrix of the master alloy particles, leading to the formation of a transient liquid phase [19,20]. As the goal of the presintering heat treatment was the homogenisation of microstructure with the help of a liquid phase that forms during sintering, heating to 400 °C and dwelling at this temperature for 20 min followed by heating to 525 °C and soaking at this temperature for 45 min was chosen as the presintering treatment.

Note that Alumix 431D is basically designed for cold compaction and sintering. High densities are difficult to achieve in the solid–state sintering of Al-based powders [21], and the effective sintering of Al and its alloys only takes place through the production of liquid phases during sintering. These liquid phases dissolve and penetrate into the oxide layer normally covering Al-based powder particles [15]. As a result, metal-to-metal contact points are developed, and alloying and densification occur. Considering all of the above, there should exist a component that produces the liquid phase(s) during sintering. In the case of Alumix 431D, the low-temperature eutectic reaction occurring in the master al-loy particles produces the liquid phase during sintering, which then promotes the sintering process [22].

3.2. Powder compacts

Fig. 2 illustrates the cross-section microstructures of various powder compacts, showing that heat treatment prior to extrusion has a great effect on microstructure. In the green (GC) compact (Fig. 2(a) and (b)), particles of Al and master alloy are easily differentiable by SEM in BSE mode.

In these micrographs, master alloy particles appear light grey and have a very fine cellular microstructure. A network of white phases is clearly visible in the microstructure of the master alloy powder particles. White phases are enriched with alloying elements (Zn, Mg, and Cu) which, in BSE mode, results in a good contrast with the adjacent Al solid solution (Al (α)) matrix. The width of the white phases is related to the size of the master alloy particles and varies from a few hundred nanometres in the very small particles to a few microns in the largest ones. Neikov et al. [23] have reported a similar microstructure for the pre-alloyed Al–Zn–Mg–Cu powders produced by atomisation.

The Al particles appear dark grey and show no specific features. The etched microstructure of the GC compact is presented in Fig. 3. The average grain size of the Al particles is related to the size of the powder particles and, as a direct consequence, is dependent on the cooling rate. Here, the average grain size ranges from a few microns for the small Al particles to approximately 20–30 μm for the largest ones.

Al and master alloy particles are still recognisable in the delubricated (DL) compact (Fig. 2(c)). Here, the appearance of the intermetallic phases dispersed within the master alloy particles differs from that of the GC sample (Fig. 2(a) and (b)); they are larger and fewer in number. It seems likely that heating to 400 °C and soaking at this temperature caused their growth.

Compared with the GC and DL samples, the presintered (PS) compact (Fig. 2(d)) has a completely different microstructure. As illustrated here, after the presintering treatment, a homogeneous distribution of intermetallic phases was found throughout the microstructure, and Al and master alloy particles were no longer distinguishable. Additionally, the detection of the initial interfaces of powder particles became difficult as the powder particles appear to be welded together. This microstructure was developed by the low-temperature reactions occurring in the master alloy particles. These reactions produce a liquid phase at approximately 475 °C (Fig. 1). This liquid phase can penetrate and diffuse into the Al particles. Consequently, alloying occurs and intermetallic phases precipitate during the cooling step.

The XRD patterns of the GC, DL, and PS compacts are presented in Fig. 4. Analysis of the XRD patterns determined that the white phases present in the microstructure of the GC compact are mainly Mg_{32} (Al, Zn)$_{49}$ (the T phase). This phase is a metastable phase of Al–Zn–Mg and Al–Zn–Mg–Cu alloying systems that can be pro-duced through rapid solidification. Considering the high cooling rate in atomisation, the presence of this phase in atomised master alloy particles is predictable. Other researchers have also con-firmed that the nonequilibrium eutectic structure in Al–Zn–Mg–Cu alloys is mainly composed of the Al (α) (Al solid solution) and T (Mg_{32} (Al, Zn)$_{49}$) phases [19,20].

After either the delubrication or presintering heat treatments, $MgZn_2$ was the major intermetallic phase detectable in the microstructure. However, the morphology and size of the $MgZn_2$ phases present in the microstructures of the DL and PS compacts are rather different. It seems likely that the $MgZn_2$ phase in the DL sample has originated from the metastable T phase, which transformed into this stable compound during delubrication. The growth of the intermetallic phases at high temperature is also possible. In contrast, the $MgZn_2$ phase in the PS sample has precipitated from the Al solid solution developed by presintering heat treatment and has grown during the cooling step.

The cross-section microstructure and XRD pattern of the GC compact heated to extrusion temperature (425 ° C) and water quenched are displayed in Fig. 5. The microstructure of the water-quenched GC compact (Fig. 5(a)) is quite similar to that of the DL sample (Fig. 2(c)). The XRD pattern (Fig. 5(b)) also indicates that the water-quenched GC compact contains the $MgZn_2$ phase, thus verifying that the transformation of the metastable T phase (Mg_{32} (Al, Zn)$_{49}$) to the stable $MgZn_2$ compound takes place during heating to either delubrication or extrusion temperature. Never-theless, the starting temperature and sequence of this transforma-tion is not known.

The as-compacted and as-water-quenched hardness values of the GC, DL, and PS powder compacts are shown in Table 1.

After cold compaction, the hardness of the GC compact was 47.3 HV. Both the delubrication treatment and the heating to

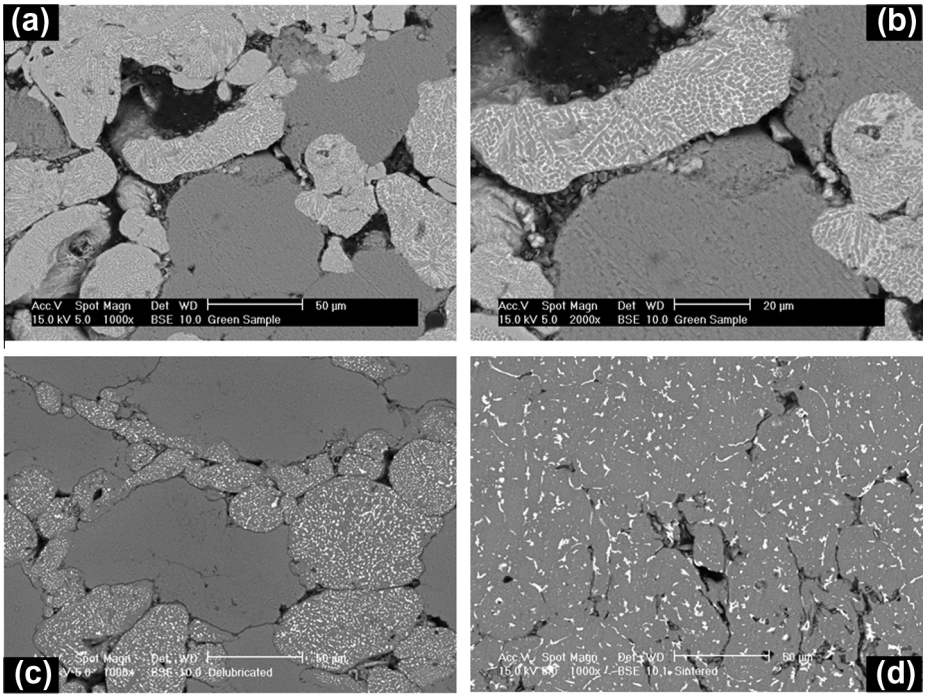

Fig. 2. Cross-section microstructures of the (a and b) green (GC), (c) delubricated (DL), and (d) presintered (PS) powder compacts.

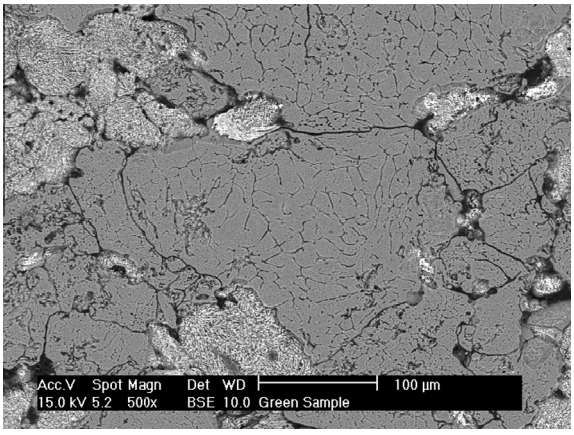

Fig. 3. Cross-section microstructure of the green (GC) compact (treated with Keller etchant).

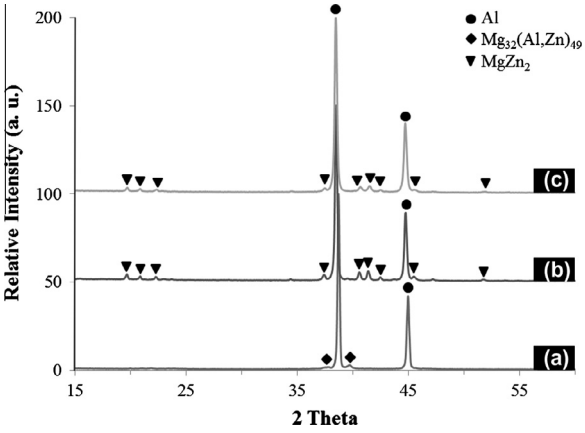

Fig. 4. X-ray diffraction (XRD) patterns of the (a) green (GC), (b) delubricated (DL), and (c) presintered (PS) powder compacts.

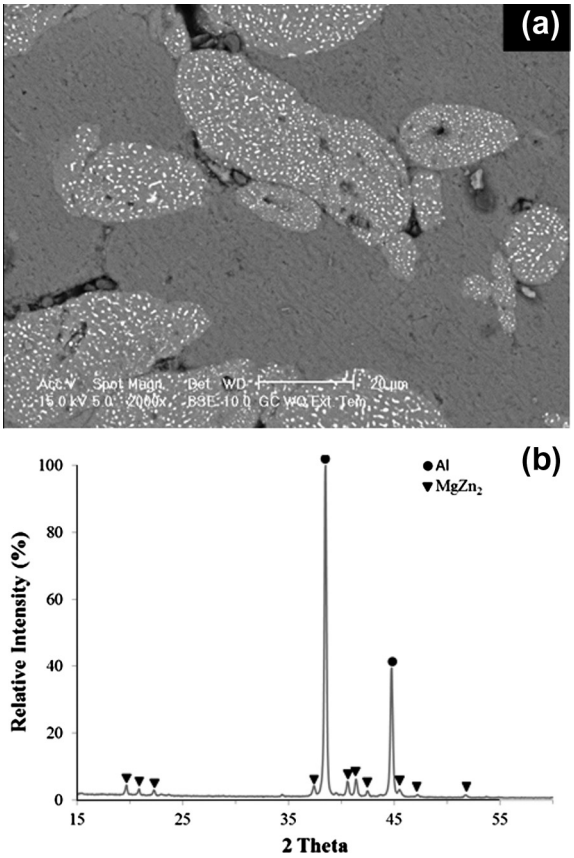

Fig. 5. (a) Cross-section microstructure and (b) X-ray diffraction (XRD) pattern of the green (GC) compact heated to 425 °C and water quenched.

extrusion temperature followed by water quenching led to a decrease in the hardness of the GC compact. Just as the microstructures of the DL and water-quenched GC compacts appear quite

Table 1
Vickers hardness values (HV10) of different powder compacts.

Compact	Hardness (HV10) (as-compacted)	Hardness (HV10) (as-water quenched)
GC	47.3 ± 1.7	37.7 ± 2.1
DL	36 ± 1.3	59 ± 2
PS	53.6 ± 1.4	81.3 ± 1.5

similar, their hardness values are also very close. The growth of grains and intermetallic phases, oxidation, and the activation of restoration mechanisms are the likely factors responsible for this hardness reduction. In contrast to the DL compact, the PS compact is harder than the GC compact. This hardness increase can be attributed to the penetration of the liquid phase into the Al particles and the formation of an Al solid solution (Al (α)), yielding a homogeneous distribution of hard intermetallic phases in the microstructure and causing bonding between the powder particles, which strengthens the material. Except for the GC compact, heating to extrusion temperature and water quenching resulted in a remarkable increase in hardness. As the heating to extrusion temperature was slow (at heating rate of 3 °C/min), there was sufficient time for the intermetallic phases to dissolve into the neighbouring Al matrix and form a saturated Al solid solution. Water quenching kept the alloying elements in solution, and hardness increased through solid solution strengthening.

A comparison of the microstructures of the as-presintered and as-water-quenched PS compacts confirms the dissolution of intermetallic phases in the neighbouring Al matrix and the formation of a saturated solid solution (Fig. 6). The described mechanism was less effective for the water-quenched DL sample. In the DL compact, all of the intermetallic phases are located in the master alloy particles (Fig. 2(c)). The matrix of the master alloy particles is an Al solid solution with a high content of alloying elements. Therefore, the dissolution of intermetallic phases and their incorporation into the highly saturated Al solid solution matrix of the master alloy particles is more difficult. Fig. 7 compares the microstructure of the as-delubricated and as-water-quenched DL compacts. It is evi-dent that the degree of solution of the intermetallic phases into the neighbouring Al matrix is less than that for the water-quenched PS sample. The diffusion of alloying elements from master alloy particles into adjacent Al particles and formation of an Al solid solution (alloying) may also account for the observed increase in the hardness of the water-quenched DL compact.

In the case of the water-quenched GC compact, it appears that the mentioned strengthening mechanism could not compensate for the hardness reduction caused by factors such as the growth of grains and intermetallic phases, oxidation, and the activation of restoration mechanisms. Thus, the hardness of the GC compact decreased during its heating to extrusion temperature.

3.3. Extrusion of powder compacts

The loads required for the extrusion of the green and heat-treated compacts are listed in Table 2. We observed a direct relationship between the hardnesses of the as-water-quenched compacts and their extrusion loads. As-water-quenched compacts with higher hardness required higher loads for extrusion. It is generally believed that there is a direct relationship between the hardness of an extrusion billet and the extrusion load. As in the present case,

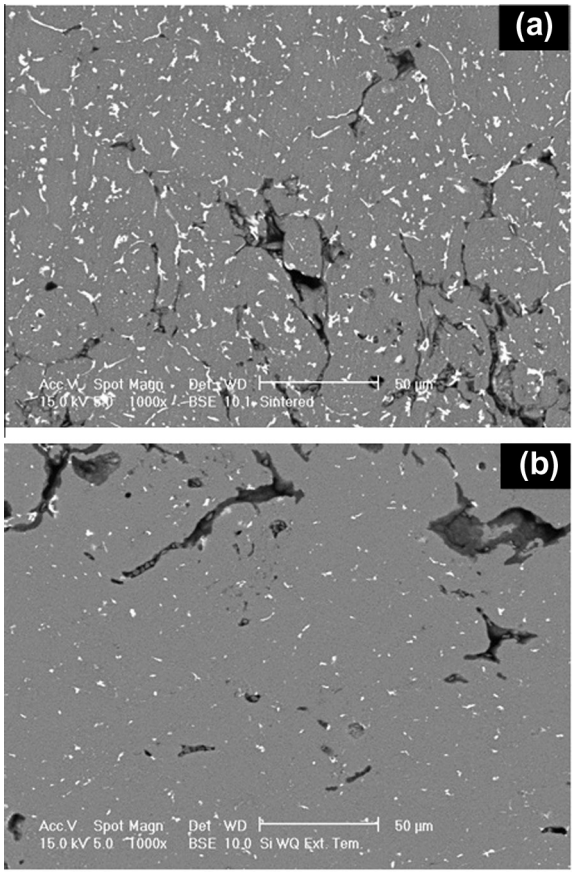

Fig. 6. Cross-section microstructures of the (a) as-presintered and (b) as-water-quenched presintered (PS) powder compacts.

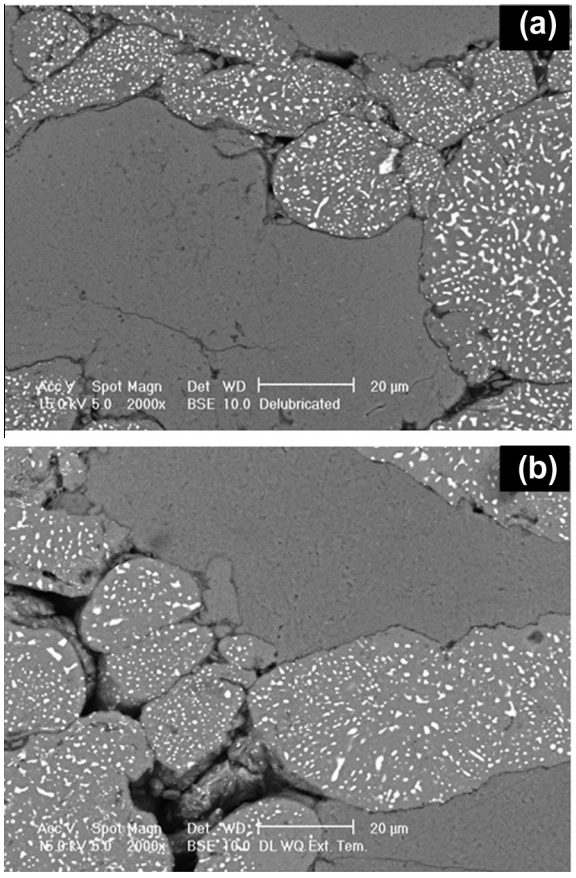

Fig. 7. Cross-section microstructures of the (a) as-delubricated and (b) as-water-quenched delubricated (DL) powder compacts.

Table 2
Extrusion loads required for the extrusion of different powder compacts.

Compact	Extrusion load (kN)
GC	139
DL	158
PS	182

the billet may experience microstructural changes during heating to extrusion temperature. In these cases, the microstructural changes during heating to extrusion temperature and their effect on mechanical properties should also be considered in the extrusion process.

3.4. Extruded materials

The longitudinal section microstructures of the extruded materials are illustrated in Fig. 8. No porosity was present in the microstructures of the extruded samples. Therefore, the used extrusion ratio was sufficiently high to produce full-density bulk materials from powder compacts. The microstructures of the GC and DL extrudates (Fig. 8(a) and (c)) are characterised by a banded (layered) structure consisted of repeating bands filled with white second phase particles (white bands) and bands containing almost no second phase (grey bands). In other words, banding of the intermetallic phases parallel to the extrusion direction was observed. It seems likely that the white bands originated from master alloy particles present in the GC and DL powder compacts, whereas the grey bands were apparently formed from the Al particles. A comparison of the EDS analyses of the Al and master alloy particles with those of the grey and white bands supported this interpretation (data not shown). Furthermore, the second phase particles present in the white bands of the GC and DL extrudates are very similar in size and shape to those present in the master alloy particles of the water-quenched GC and DL compacts.

Banding phenomena normally occur in the extrusion of powder mixtures containing components with different hardnesses and flow stresses. In this case, the components show different deformation behaviours during extrusion. Softer components undergo more deformation than do harder components. As a result, less-deformed components align with the extrusion direction to form bands. For example, Dobrzanski et al. observed banded structures in Al matrix composites consolidated from powder mixtures containing an Al-based powder (EN AW-2124) and ceramic reinforcements (Al_2O_3 and BN) by extrusion [24]. They concluded that extrusion could align reinforcement particles along the extrusion direction, thus resulting in bands filled with reinforcement particles.

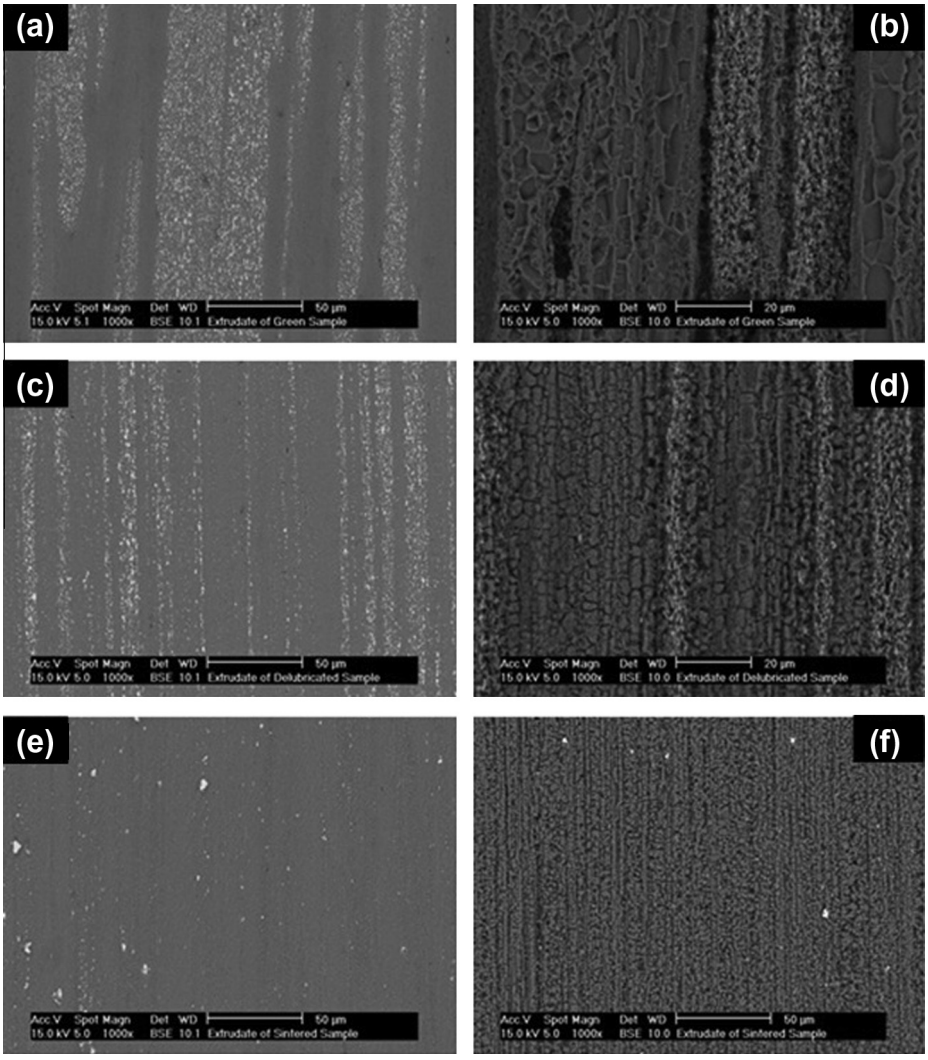

Fig. 8. Longitudinal section microstructures of the extrudates consolidated from (a and b) green (GC), (c and d) delubricated (DL), and (e and f) presintered (PS) powder compacts.

The master alloy particles, which are recognisable in the GC and DL compacts (Fig. 2(a) and (c)) and even in the GC and DL compacts water quenched from extrusion temperature (Figs. 5(a) and 7(b)), contain a large amount of alloying elements. This led to a high hardness for the master alloy particles (105 HV) while the hardness of the Al particles was measured to be 29 HV. The remarkable difference between the hardnesses of Al and master alloy particles resulted in the different flow stresses and deformation behaviours of each particle type during the extrusion process. Therefore, banded structures developed during the extrusion of the GC and DL powder compacts.

In contrast to the GC and DL extrudates, the banded structure is much less visible in the PS extrudate (Fig. 8(e)). As shown in Fig. 2(d), the PS compact has a homogeneous microstructure in which the former Al particles are now indistinguishable from the master alloy particles. All of the particles seem to have undergone the same amount of deformation during extrusion, probably due to the fact that they all have the same hardness, and as a conse-quence, almost no banding occurred. There is a homogeneous dis-tribution of the fine second phase particles in the microstructure of the PS extrudate. However, some isolated larger second phase par-ticles are also seen. Considering the high extrusion ratio employed (25:1), the fracturing of the intermetallic phases present in the microstructure of the water-quenched PS compact (Fig. 6(b)) during extrusion is predictable, thus leading to the formation of the fine second phase particles. Moreover, a large amount of the intermetallic phases present in the microstructure of the PS compact dissolve into surrounding Al matrix during heating to extrusion temperature (Fig. 6). Therefore, dynamic precipitation during extrusion and static precipitation after extrusion during the air cooling step are also probable sources of the fine intermetallic phases present in the microstructure of the PS extrudate. Larger precipitates may have originated from less-deformed intermetallic phases or from the growth of second phase nuclei during the cooling step.

The effects of heat treatment prior to extrusion on the grain structures of the extruded materials are displayed in Fig. 8(b),(d), and (f) (treated with Keller etchant). There are two distinct re-gions in the GC and DL extrudates. The first region corresponds to the white bands visible in Fig. 8(a) and (c), which have high intermetallic phase contents. This region consists of submicron equiaxed grains, which is considered to be a highly recrystallised grain structure. According to McQueen et al. [25], dynamic recov-ery (DRV) results in large, elongated grains with an internal equi-axial subgrain structure, whereas dynamic recrystallisation (DRX) results in new equiaxed grains. Due to their high stacking fault energies, Al alloys show a very high rate of DRV during hot deformation. As a result, DRX may be completely prevented. However, as seen here, recrystallisation can occur during the extrusion of powder compacts that are cold pressed from a premixed Al–Zn–Mg–Cu powder. Recrystallisation and formation of new grains during hot deformation of Al alloys have also been reported by other researchers. Blum et al. [26] carried out hot torsion tests on AA 5083 Al alloy and observed a refined and nearly equiaxed grain structure developed by geometric dynamic recrystallization. Also, Gourdet and Montheillet [27] submitted various Al specimens (three types of polycrystalline Al: a high purity Al (1199), a commercial purity Al (1200), and an Al–2.5 wt.% Mg alloy (AA 5052)) to uniaxial compression and torsion testing. They related the observed grain structures to simultaneous occurrence of geometric and continuous dynamic recrystallization.

The second region in the GC and DL extrudates contains large and elongated grains along the extrusion direction. Some equiaxed grains are also detectable in this region. This structure is the result of the simultaneous occurrence of DRV and DRX. This region corresponds to the grey bands in Fig. 8(a) and (c), namely, the Al bands.

As the second phases dispersed in the white bands of GC and DL extrudates are much harder than the surrounding Al matrix, they generally do not experience as much deformation as the Al matrix undergoes during extrusion. Additionally, the second phases can impose extra deformation on the zones surrounding them. These highly deformed zones are susceptible to the nucleation of new grains. Therefore, second phase particles can encourage recrystallisation. A similar effect has been reported for the reinforcement particles in powder-processed metal matrix composites consolidated by extrusion [28]. In addition to the second phase particles, white bands, which originated from the master alloy particles in the GC and DL compacts, contain large amounts of alloying elements dissolved in the Al solid solution matrix of these bands. Therefore, interactions between the alloying elements in solution and restoration mechanisms should also be considered. Alloying elements (especially Mg) can retard DRV by reducing the stacking fault energy of Al. In addition, dislocation mobility, which is necessary for recovery to occur, can be reduced by the solute drag effect of alloying elements [25]. Therefore, alloying elements in solid solution can hamper recovery and, as a direct consequence, promote recrystallisation. Larger amounts of alloying elements in solution before extrusion thus yield higher degrees of recrystallisation during and after extrusion. Considering all of the above, the submicron grain structure of the white bands of the GC and DL extrudates can be attributed to the recrystallisation-promoting effect of the second phase particles and the alloying elements in solution.

DRV appears to be the dominant restoration mechanism acting in the Al bands of the GC extrudate, whereas both DRV and DRX seem to be active in the Al bands of the DL extrudate. This difference can be related to the different degrees of alloy development for the Al particles present in the GC and DL compacts, subsequently forming the grey bands of the GC and DL extrudates during extrusion. Compared with the GC compact, the Al particles of the DL compact may contain more alloying elements in solution as alloying elements in solution can promote DRX during extrusion.

In contrast to the GC and DL samples, the PS extrudate shows a homogeneous grain structure composed of fine equiaxed grains. The size of the grains ranges from submicron to a few microns. Fig. 9 shows the longitudinal section microstructures of the centre and periphery of the PS extrudate. As the periphery experiences more deformation during extrusion, it can accordingly be seen that the grains in this zone are finer than those at the centre of the extrudate. As shown, the PS extrudate exhibits a highly recrystallised grain structure in all zones.

The recrystallised microstructure of the PS extrudate can be attributed to the microstructure of the water-quenched PS compact (Fig. 6(b)). This compact consists of powder particles containing intermetallic phases homogeneously distributed in the Al solid solution matrix of the particles. The Al matrix of the particles also has a significant amount of alloying elements in solution. The second phase particles present in the microstructure, along with the alloying elements in solution, retard recovery and favour recrystallisation during and after extrusion. Furthermore, the growth of recrystallised grains is hindered by the fine second phase particles and precipitates. The high strains and shear stresses involved in the extrusion process can break the second phase particles into finer ones.

Fig. 10 presents the XRD patterns of the GC, DL, and PS extrudates, indicating that $MgZn_2$ is the major intermetallic phase present in the microstructures of these extrudates. As this phase was also the major intermetallic phase present in the microstructures of the powder compacts (Figs. 4(b) and (c) and 5(b)), we concluded that extrusion at 425 °C had no significant influence on the composition of the intermetallic phases present in the microstructure. Only the fracture of intermetallic particles may occur during

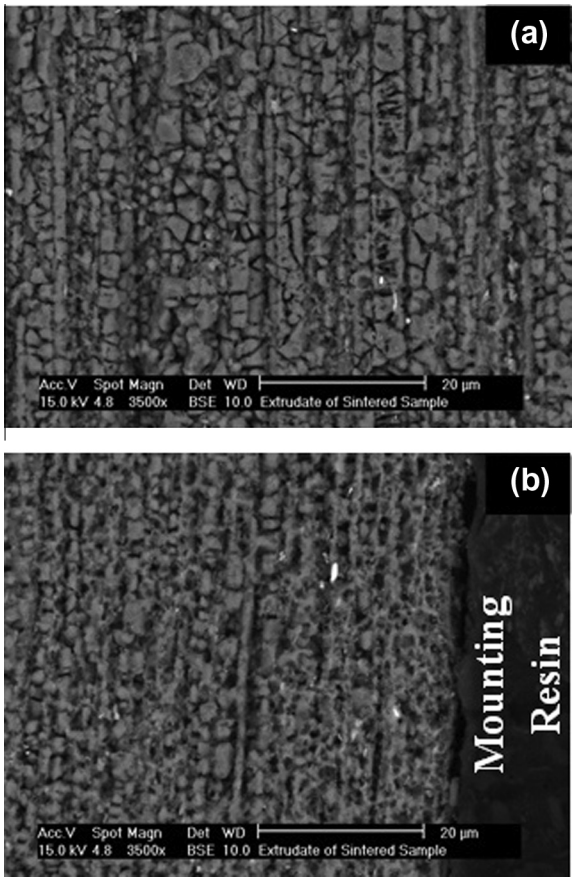

Fig. 9. Longitudinal section microstructures of the (a) centre and (b) periphery of the presintered (PS) extrudate.

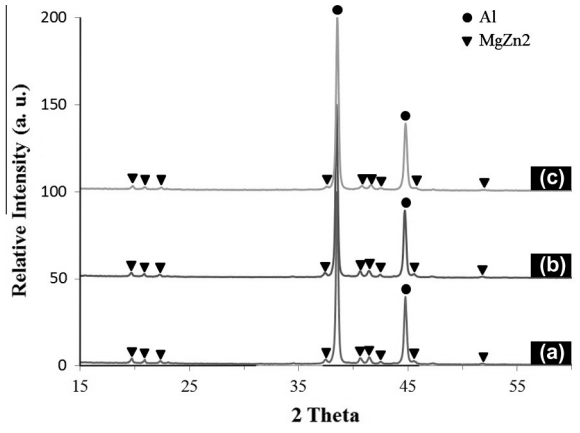

Fig. 10. X-ray diffraction (XRD) patterns of the extrudates consolidated from (a) green (GC), (b) delubricated (DL), and (c) presintered (PS) powder compacts.

extrusion. In addition, the precipitation of fine intermetallic phases from the saturated Al solid solution matrix, which contains a large amount of alloying elements in solution, may occur during extrusion and air cooling from extrusion temperature.

The hardness values of the extruded materials are presented in Table 3, indicating that the extrusion process significantly increased the hardnesses of the samples. Densification attained through extrusion is considered to be the main hardening factor. We found that, regardless of the heat treatment prior to extrusion, no porosity was present in the microstructures of the extruded materials, which therefore resulted in high tensile elongations for all of the processed alloys. The elimination of porosity by the extrusion process can effectively enhance the hardness of the extrusion products. The observed increases in hardness through extrusion can also be attributed to the work hardening effect associated with the extrusion process.

Table 3
Mechanical properties of the extruded alloys.

Extrudate	Hardness (HV10)	Yield strength (MPa)	Tensile strength (MPa)	Elongation (%)	Compressive strength (MPa)
GC	80.6 ± 1.8	213 ± 11	331 ± 15	8.6 ± 0.5	359 ± 9
DL	82.8 ± 1.6	229 ± 15	338 ± 13	9.2 ± 0.4	369 ± 5
PS	94 ± 1.7	307 ± 17	450 ± 20	8.9 ± 0.5	471 ± 12

Table 3 also shows that the mechanical properties of the processed alloys are highly dependent on the degree of alloy development in powder compacts. A higher degree of alloy development prior to extrusion leads to higher as-extruded mechanical properties. The degree of alloy development for the DL powder compact is almost similar to that for the GC powder compact, leading to similar microstructures and mechanical properties for the GC and DL extrudates. However, the mechanical properties of these extrudates are remarkably lower than those of the PS extrudate, which can be attributed to their banded structures and coarser grains.

The PS powder compact presents the highest degree of alloy development prior to extrusion, which results in excellent mechanical properties for the PS extrudate. Higher degrees of alloy development mean higher incorporation of alloying elements into the Al solid solution matrix, which can enhance the mechanical properties of the extruded alloy through solid solution strengthening. Moreover, the PS extrudate shows an ultrafine, recrystallized grain structure and a homogeneous distribution of fine second phase particles in the microstructure, which can improve its mechanical properties through the combined effects of grain-size and dispersion strengthening.

4. Conclusions

In this study, 7075 Al alloy was processed by cold compaction and direct hot extrusion of a premixed powder. Due to their favourable compressibility and deformability, PM Al premixes are believed to have an excellent potential as the starting material for hot deformation processes such as powder extrusion and forging. The main conclusions derived from this study are the following:

(1) Using Alumix 431D premix as the starting material, the heat treatment prior to extrusion has a significant effect on the degree of alloy development in powder compacts. Different degrees of alloying are obtainable through such mechanisms as solid-state diffusion of alloying elements from the master alloy particles into the Al particles and the formation of a low-temperature liquid phase in the master alloy particles and its subsequent penetration into the Al particles. Higher degrees of alloy development prior to extrusion result in higher extrusion loads and as-extruded mechanical properties.
(2) Banded structures consisting of two repeating bands are observed in the extrudates consolidated from the GC and DL powder compacts, in which the master alloy and Al particles are distinguishable. Remarkable differences between the microstructures and hardnesses of the master alloy and the Al particles account for the development of banded structures through the extrusion process.

(3) The dominant restoration mechanism during extrusion is highly dependent on the heat treatment prior to extrusion and the resulting degree of alloy development. Depending on the degree of alloy development prior to extrusion, recovery and/or recrystallisation may occur during extrusion. A higher degree of alloy development prior to extrusion leads to more recrystallisation during extrusion. This can be attributed to the promoting effects of the alloying elements in solid solution and the second phase particles dispersed in the microstructure on recrystallisation.

(4) The extrusion process significantly enhanced the hardnesses of the samples. This was attributed partly to densification, which is achieved by extrusion, and partly to the work hardening effect associated with the extrusion process.

(5) Thanks to a recrystallized grain structure and the homogeneous distribution of fine second phase particles in its microstructure, the extrudate consolidated from the PS powder compact shows excellent mechanical properties, which are far better than those of the GC and DL extrudates.

Acknowledgments

The authors would like to thank the Comunidad de Madrid for their financial support of this work through the ESTRUMAT Grant #S2009/MAT-1585.

References

[1] Jin N, Zhang H, Han Y, Wu W, Chen J. Hot deformation behavior of 7150 aluminum alloy during compression at elevated temperature. Mater Charact 2009;60:530–6.

[2] Rokni MR, Zarei-Hanzaki A, Roostaei AA, Abolhasani A. Constitutive base analysis of a 7075 aluminum alloy during hot compression testing. Mater Des 2011;32:4955–60.

[3] Yang Y, Zhang Z, Li X, Wang Q, Zhang Y. The effects of grain size on the hot deformation and processing map for 7075 aluminum alloy. Mater Des 2013;51:592–7.

[4] Rokni MR, Zarei-Hanzaki A, Roostaei AA, Abedi HR. An investigation into the hot deformation characteristics of 7075 aluminum alloy. Mater Des 2011;32:2339–44.

[5] MacAskill IA, LaDepha ADP, Milligan JH, Fulton JJ, Bishop DP. Effects of cold and hot densification on the mechanical properties of a 7xxx series powder metallurgy alloy. Powder Metall 2009;52:304–10.

[6] Schatt W, Wieters KP. Powder metallurgy: processing and materials. Shrewsbury (UK): European Powder Metallurgy Association; 1997.

[7] Verlinden B, Froyen L. TALAT lecture 1401: aluminum powder metallurgy. Brussels (Belgium): European Aluminium Association; 1994.

[8] Torralba JM, Lancau V, Martínez MA, Velasco F. P/M aluminum matrix composite reinforced with (AlCr2)p. J Mater Sci Lett 2000;19:1509–12.

[9] Fogagnolo JB, Robert MH, Ruiz-navas EM, Torralba JM. Extrusion of mechanically milled composite powders. J Mater Sci 2002;37:4603–7.

[10] Fogagnolo JB, Robert MH, Ruiz-Navas EM, Torralba JM. 6061 Al reinforced with zirconium diboride particles processed by conventional powder metallurgy and mechanical alloying. J Mater Sci 2004;39:127–32.

[11] Adamiak M, Fogagnolo JB, Ruiz-Navas EM, Dobrzañski LA, Torralba JM. Mechanically milled AA6061/(Ti3Al)P MMC reinforced with intermetallics - the structure and properties. J Mater Process Technol 2004;155–156:2002–6.

[12] Velasco F, Da Costa CE, Candela N, Torralba JM. Fracture analysis of aluminium matrix composite materials reinforced with (Ni3Al)p. J Mater Sci 2003;38:521–5.

[13] Fogagnolo JB, Ruiz-Navas EM, Robert MH, Torralba JM. 6061 Al reinforced with silicon nitride particles processed by mechanical milling. Scr Mater 2002;47:243–8.

[14] Song M, Y-h He. Effects of die-pressing pressure and extrusion on the microstructures and mechanical properties of SiC reinforced pure aluminum composites. Mater Des 2010;31:985–9.

[15] Martin JM, Castro F. Liquid phase sintering of P/M aluminium alloys: effect of processing conditions. J Mater Process Technol 2003;143–144:814–21.

[16] Min KH, Kang SP, Lee B-H, Lee J-K, Kim YD. Liquid phase sintering of the commercial 2xxx series Al blended powder. J Alloys Compd 2006;419:290–3.

[17] Schaffer GB, Huo SH. Distortion in a sintered 7000 series aluminium alloy. Powder Metall 2000;43:163–7.

[18] Zubizarreta C, Giménez S, Martín JM, Iturriza I. Effect of the heat treatment prior to extrusion on the direct hot-extrusion of aluminium powder compacts. J Alloys Compd 2009;467:191–201.

[19] Yuan W, Zhang J, Zhang C, Chen Z. Processing of ultra-high strength SiCp/Al–Zn–Mg–Cu composites. J Mater Process Technol 2009;209:3251–5.

[20] Belov NA, Eskin DG, Aksenov AA. Multicomponent phase diagrams: applications for commercial aluminum alloys. Amsterdam: Elsevier; 2005.

[21] Schaffer GB, Sercombe TB, Lumley RN. Liquid phase sintering of aluminium alloys. Mater Chem Phys 2001;67:85–91.

[22] Gradl J, Neubing HC, Muller A. Improvement in the sinterability of 7-xxx-based aluminium premix. Euro PM2004. Vienna, Austria; 2004. p. 13–21.

[23] Neikov OD, Vasilieva GI, Sameljuk AV, Krajnikov AV. Water atomised aluminium alloy powders. Mater Sci Eng A 2004;383:7–13.

[24] Dobrzanski, Leszek A, Wlodarczyk A, Adamiak M. The structure and properties of PM composite materials based on EN AW-2124 aluminum alloy reinforced with the BN or Al_2O_3 ceramic particles. J Mater Process Technol 2006;175:186–91.

[25] McQueen HJ, Evangelista E, Kassner ME. Classification and determination of restoration mechanisms in the hot working of Al alloys. Mater Res Adv Technol 1991;82:336–45.

[26] Blum W, Zhu Q, Merkel R, McQueen HJ. Geometric dynamic recrystallization in hot torsion of Al—5Mg—0.6Mn (AA5083). Mater Sci Eng A 1996;205:23–30.

[27] Gourdet S, Montheillet F. An experimental study of the recrystallization mechanism during hot deformation of aluminium. Mater Sci Eng A 2000;283:274–88.

[28] Shahani RA, Clyne TW. Recrystallization in fibrous and particulate metal matrix composites. Mater Sci Eng A 1991;135:281–5.